

# Conceptual Design of Magnets with CIC Conductors for LHD-type Reactors FFHR2m

Shinsaku IMAGAWA, Akio SAGARA and Yasuji KOZAKI

*National Institute for Fusion Science, 322-6 Oroshi, Toki, Gifu 509-5292, Japan*

(Received 17 November 2007 / Accepted 29 January 2008)

LHD-type reactors have attractive features for fusion power plants, such as no requirement of a current drive and a wide space between the helical coils for the maintenance of in-vessel components. One disadvantage was considered the requirement of a large major radius to attain the self-ignition condition with a sufficient space for blankets. According to the recent reactor studies based on experimental results in LHD, the major radius of plasma is set at 14 to 17 m with the central toroidal field of 6 to 4 T. The stored magnetic energy is estimated at 120 to 130 GJ. Both the major radius and the magnetic energy are about three times as large as those for ITER. We intend to summarize the requirements for superconducting magnets of the LHD-type reactors and propose a conceptual design of the magnets with cable-in-conduit (CIC) conductors based on the technology for ITER.

© 2008 The Japan Society of Plasma Science and Nuclear Fusion Research

Keywords: cable-in-conduit conductor, fusion reactor, helical coil, LHD, superconducting magnet.

DOI: 10.1585/pfr.3.S1050

## 1. Introduction

Superconducting magnets for fusion reactors should have high mechanical strength, high reliability, and low costs as well as sufficient current densities in high fields. Cable-in-conduit (CIC) conductors have been developed for large pulse coils, and they are adopted for all magnets of ITER [1–3]. Major features of the CIC conductors are a large current up to 100 kA, high strength with thick conduits, small AC losses, and high cryogenic stability. One disadvantage is that the necessity of circulation pumps for forced-flow cooling. The maximum length of the cooling path is about 500 m, determined by the pressure drop at the required mass flow against nuclear heating. A CIC conductor will not be the best for magnets of a helical reactor operated with a constant current. However, technology related to the CIC conductors will be strongly improved through the construction of ITER, especially in cost and the winding technique. Further, their features of high strength and large currents are suitable for large magnets for helical reactors. Therefore, we study a helical winding with CIC conductors using ITER technology as a conventional option.

## 2. Magnet Systems of an LHD-type Reactor

A magnet system of an LHD-type reactor consists of a pair of continuous helical coils and more than one pair of poloidal coils [4]. The position of the poloidal coils is determined by the dipole magnetic field, the quadrupole magnetic field, stray field, position of ports, etc. At least one set of poloidal coils is necessary to adjust the major

radius of the plasma, quadrupole field, and stray field. In this case, the magnetic field around the machine center is high, and the stored magnetic energy is large. Two pairs of poloidal coils are appropriate, because they can reduce the total weight of supporting structures with reduction of the stored magnetic energy. In addition, the position of plasma axis can be controlled without increasing the stray field. The position of the coils is not determined uniquely by the above restrictions because of the rest of the degrees of freedom. The coil position can be adjusted to attain the space for the blanket, mechanical support, and ports. In this study, we adopt two additional restrictions that  $a_{IV} = a_{OV}$  and  $Z_{IV} = Z_{OV}$ , where  $a$  is the distance from the major radius circle of the helical coils, and  $Z$  is the height, as shown in Fig. 1.

The lead angle of the helical coils is defined as the pitch parameter  $\gamma = (ma_c)/(lR_c)$ , where  $l$ ,  $m$ ,  $R_c$ , and  $a_c$  are the pole number, pitch number, coil major radius, and coil minor radius, respectively. Figure 2 shows the normalized magnetic energy of the LHD-type reactors with two sets of poloidal coils. Since the poloidal coils cancel the vertical field of the helical coils, the magnetic energy increases with increasing distance between the poloidal coils. It also increases with increasing  $\gamma$  because the toroidal field area increases with increasing  $\gamma$ .

The coil current density  $j$  is very important for the design of superconducting magnets. Although the high density is useful to enlarge the space for blankets and ease of maintenance, it is restricted by cryogenic stability, mechanical strength, and the maximum field. Considering the space for structural materials inside the winding,  $j$  is set approximately 25 A/mm<sup>2</sup> in this study. The highest mag-

author's e-mail: [imagawa@LHD.nifs.ac.jp](mailto:imagawa@LHD.nifs.ac.jp)

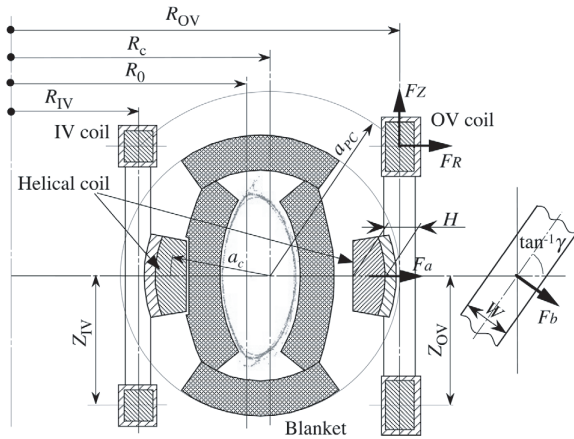


Fig. 1 Magnets and supporting structures of an LHD-type fusion reactor.

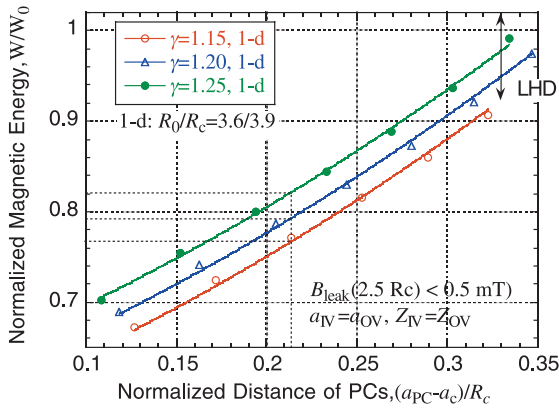


Fig. 2 Magnetic energy of LHD-type reactors with two pairs of poloidal coils. It is normalized to the magnetic energy using helical coils with  $\gamma$  of 1.15 at the same central toroidal field.

netic field is also important for the superconducting magnets. The ratio of the highest field to the central toroidal field depends mainly on the ratio of the height of the helical coils to  $a_c$  [5]. The design criterion stipulates the highest field to be less than 13.5 T, the same as the ITER-CS coils.

The necessary magnetic field and size can be determined by the scaling law for plasma confinement and the necessary space for blankets. The scaling law of ISS04 [6] is adopted in this study. First, we studied the necessary size to satisfy the self-ignition condition in the case that the enhancement factor of energy confinement is 1.12 in the ISS04 scaling. Since LHD has attained a factor of 0.93, the required further improvement is a factor of 1.2 that can be achieved in the near future. The other design conditions in this parameter study are the minimum space for blankets of 1.1 m and the helical coil current density of 20-30 A/mm<sup>2</sup>. The assumptions required to estimate the fusion power are as follows: a parabolic distribution for both the plasma density and temperature, helium ash ratio of 3%,

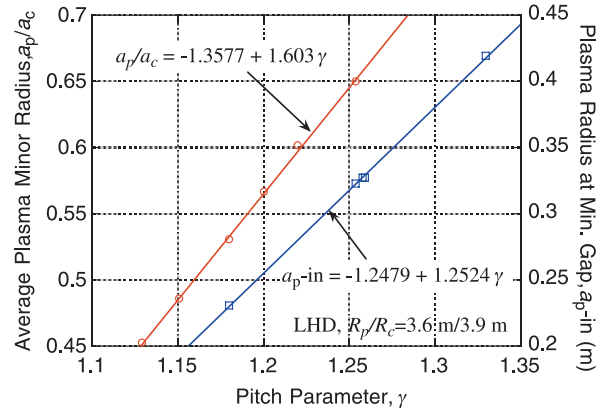


Fig. 3 Average plasma radius and the plasma radius at the position of the minimum gap in the helical coils of LHD.

oxygen impurities ratio of 0.5%, and alpha particle heating ratio of 90%. The plasma density was set to the density limit of the Sudo scaling [7]. The central temperature was adjusted to adjust the average  $\beta$ , the ratio of plasma pressure to the central magnetic pressure, to 5%. According to the ISS04 scaling, high-density operations increase the energy confinement time. Therefore, the enhancement factor is less with the higher  $\beta$  operation in which the larger fusion power is produced.

The plasma shape is assumed to be similar to that of LHD at the inward shift mode, in which the best plasma confinement has been achieved. We use the same ratio of the average plasma minor radius  $a_p$  to the coil minor radius as LHD, as shown in Fig. 3. Since the plasma radius is almost independent of the current density of the helical coil, the minimum gap for blanket,  $\Delta_d$ , is derived as,

$$\Delta_d = a_c - a_{p-in} - H/2 - 0.1, \quad (1)$$

where  $a_{p-in}$  is the inward plasma radius at the position where the plasma is vertically elongated and the blanket space is the narrowest. The last term of 0.1 m is the space for thermal shields.

In the above conditions, the smallest major radius is determined mainly by the space for blankets, rather than the highest magnetic field. Table 1 shows typical examples of the design parameters of the FFHR2m2 in the case of  $j = 27.5$  A/mm<sup>2</sup>. In addition, the effects of  $\gamma$  and  $j$  on the major parameters are shown in Fig. 4. Although the coil major radius around 17 m is required for a reactor similar to LHD, the stored energy is in the range of 120 to 130 GJ in the case of  $j = 25$  A/mm<sup>2</sup>. It is comparable to the conventional tokamak reactors. The major radius and magnetic energy can be reduced by increasing  $j$ . On the other hand, the maximum magnetic field on the coil increases with increasing  $j$ . In this design area, high  $j$  close to 30 A/mm<sup>2</sup> seems to be preferred to reduce the construction cost, as far as the mechanical strength can be secured. The fusion power increases with increasing  $\gamma$ , because of the increase in plasma volume. The stored energy is pro-

Table 1 Case study of LHD-type reactors FFHR2m2\_ $j$ 27.5.

	$\gamma$ 1.15	$\gamma$ 1.2	$\gamma$ 1.25
Polarity/Field periods, $l/m$	2/10	2/10	2/10
Coil pitch parameter, $\gamma$	1.15	1.20	1.25
Coil major radius, $R_c$ (m)	15.68	16.52	17.53
Coil minor radius, $a_c$ (m)	3.61	3.97	4.38
Coil center line length (m)	150	162	176
Plasma major radius, $R_0$ (m)	14.47	15.25	16.18
Plasma minor radius, $a_p$ (m)	1.75	2.24	2.83
Plasma volume, $V_p$ (m <sup>3</sup> )	877	1515	2561
Central magnetic field, $B_0$ (T)	5.53	4.95	4.49
Max. field on coils, $B_{\max}$ (T)	12.1	12.0	12.2
Coil current, $I$ (MA)	40.1	37.7	36.4
Coil current density, $j$ (A/mm <sup>2</sup> )	27.5	27.5	27.5
Blanket space, $\Delta_d$ (m)	1.1	1.1	1.1
Magnetic energy, $W$ (GJ)	128	123	126
Density, $n_e(0)$ ( $10^{19}$ m <sup>-3</sup> )	35.0	26.2	20.5
Ion temperature, $T_i(0)$ (keV)	16.9	17.9	18.9
Average beta, $\langle\beta\rangle$	5	5	5
Fusion power, $P_F$ (GW)	3.9	4.2	4.8
Energy confinement time, $\tau_E$ (s)	1.32	1.66	2.01
Enhancement factor to ISS04	1.12	1.12	1.12

Table 2 Design criteria for CIC conductors based on ITER.

Items	Design criteria	ITER-TF
Max. cooling length (m)	< 550	390
Current (kA)	< 100	68
Maximum field (T)	< 13	11.8
Non-Cu current density (A/mm <sup>2</sup> )	< 300	273
Coil current density (A/mm <sup>2</sup> )	< 30	20.3
SC material for HC	Nb <sub>3</sub> Al	Nb <sub>3</sub> Sn

### 3. Helical Coils with CIC Conductors

Main specifications of helical coils for an LHD-type reactor, FFHR2 m are as follows: a magnet-motive force of about 40 MA, a magnetic energy of 120 to 130 GJ, a coil center line of 150 to 175 m, and an average coil current density of 25 to 30 A/mm<sup>2</sup>. Design criteria for CIC conductors based on the ITER magnets are summarized in Table 2. Since the length of the coil center line of a helical coil is five times as long as that of a TF coil, some modifications are necessary in addition to adopting a large current of almost 100 kA. Parallel winding is a practical solution to shorten the cooling length within 500 m.

Two types of mechanical structures are known for CIC conductors. One is a thick conduit type, in which rectangular conductors wrapped in insulating tapes are simply wound. A high stress is induced in the insulating tapes by addition of forces on the conductors in line. The other is an internal plate type, in which conductors are wound in the grooves of the internal plate. The stress in the insulation is reduced. Besides, the force for winding is relatively small because of thin conduits. Its disadvantage is the complicated process for manufacturing internal plates. However, its technology will be improved through the construction of ITER-TF coils. Internal plates with grooves are suited for parallel winding, because CIC conductors are placed in the grooves as shown in Fig. 5. In this structure, a react-and-wind method is preferred to use a conventional insulator and to prevent huge thermal stress. Nb<sub>3</sub>Al is a candidate for the superconducting strands of the conductor because of its good tolerance against mechanical strain [8,9]. Degradation of the critical current density of Nb<sub>3</sub>Al by the axial strain of 0.4% at 12 T is only 5% in comparison with more than 30% in the case of Nb<sub>3</sub>Sn [10]. A method of react-and-wind can be adopted by managing strain during winding within about 0.5%.

The magnetic field in the helical coils is the highest in the first layer and lower in the higher layers. Therefore, the average current density of the superconducting strands can be increased by grading the conductors in the case of layer winding. Non-copper current density of Nb<sub>3</sub>Sn is given as [11],

$$j_c = 1/(1/j_{c1} + 1/j_{c0}), \quad (2)$$

$$j_{c0} = j_0 \left(1 - (T/T_{c0})^2\right), \quad (3)$$

$$j_{c1} = C_0 \left(1 - (T/T_{c0})^2\right)^2 B^{-0.5} (1 - B/B_{c2})^2, \quad (4)$$

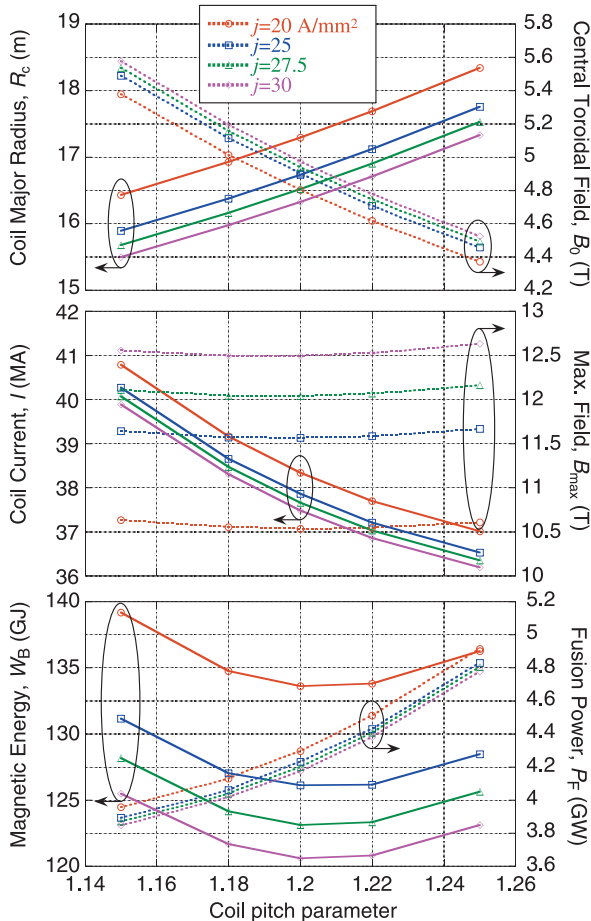


Fig. 4 Case study of LHD-type reactors FFHR2m2 for various current densities of the winding.

portional to the square of the central magnetic field and the third power of the major radius, and it decreases around  $\gamma$  of 1.2 under these conditions.

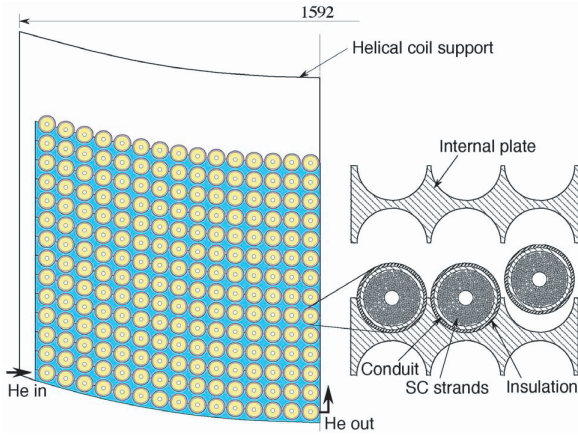


Fig. 5 Concept of helical winding with CIC conductors. The curvature of the bottom of the coil is determined to attain the maximum gap to the plasma. The helical coil support is assembled after winding.

$$B_{c2} = B_{c20} \left(1 - (T/T_{c0})^2\right) (1 - T/3T_{c0}), \quad (5)$$

$$B_{c20} = B_{c20m} (1 - a\varepsilon^{1.7}), \quad (6)$$

$$T_{c0} = T_{c0m} (1 - a\varepsilon^{1.7})^{0.333}, \quad (7)$$

where  $j$ ,  $T$ ,  $B$ , and  $\varepsilon$  are the current density, temperature, magnetic field, and strain, respectively. For ITER conductor  $j_0 = 33.51 \text{ kA/mm}^2$ ,  $T_{c0m} = 18 \text{ K}$ ,  $B_{c20m} = 28 \text{ T}$ ,  $a = 1250$  for tensile, 900 for compressive, and  $C_0 = 1150$  [3]. Figure 6 shows the non-copper current density of the strands for various magnetic fields at 7 K with the strain of  $-0.5\%$ . In the case of  $B_{\text{max}}$  of 12 T, the average current density can be increased by 60% by adopting four grades of conductors. In the case of  $\text{Nb}_3\text{Al}$  strands, a higher current density can be attained [8].

The typical design parameters of the helical coils are listed in Table 3, compared with the ITER-TF coils. By adopting large conductors of about 90 kA and the parallel winding of five-in-hand, the length of the cooling path is within 530 m including the case of  $\gamma = 1.25$  in Table 1. By increasing the number of quench protection circuits, the maximum discharge voltage can be managed to be less than 10 kV, in spite of the larger inductance and shorter discharge time constant than the ITER-TF coils. Consequently, the CIC conductors for the helical coils can be made with the same technology as for ITER.

The winding method is a critical issue for the helical coils. In the case of LHD, a special winding machine was developed. The conductors from a rotating bobbin were formed plastically into a helical shape using a shaping head near the winding guide. This method will not be compatible with the react-and-wind method, because the allowable strain is in the range of 0.5% even for  $\text{Nb}_3\text{Al}$  strands. A candidate winding method is as follows:

(1) Conductors are heated for the reaction of  $\text{Nb}_3\text{Al}$  on a bobbin the circumference of which is the same as the length of one pitch of a helical coil.

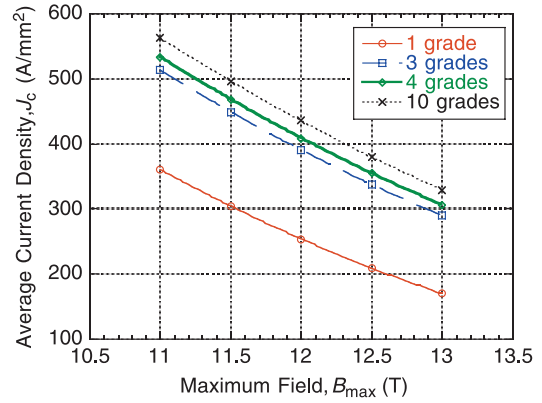


Fig. 6 Increase in non-copper current densities of superconducting strands of helical coil conductors with grading.

Table 3 Specification of a helical coil with CIC conductors.

	HC_γ1.15	HC_γ1.20	ITER-TF
Maximum field (T)	12.1	12.1	11.8
Magnetic energy (GJ)	128	124	41
Number of coils	2	2	18
Turn number per layer	30	30	11, 9, 3
Layer number per coil	14	14	10+2+2
Conductor current (kA)	95.2	89.8	68.0
Length of a cooling path (m)	450	486	390
Number of parallel winding	5	5	1
Current density ( $\text{A/mm}^2$ )	27.5	27.5	20.3
Cu ratio of strand (-)	1	1	1
Non-Cu current density ( $\text{A/mm}^2$ )	400	400	273.4
Ratio of Cu strands in area (-)	0.452	0.452	0.360
Central tube diameter (mm)	12.0	12.0	8.0
Void fraction (-)	0.34	0.34	0.34
Cable outer diameter (mm)	43.5	42.3	40.2
Conduit outer diameter (mm)	46.7	45.5	43.4
Total length of conductor (km)	126	136	82.2
Total weight of SC strands (ton)	481	490	351
Total weight of Cu strands (ton)	442	450	206
Cu current density ( $\text{A/mm}^2$ )	151	151	128.7
Discharge time constant (s)	12	12	15
Inductance (H)	28.2	30.6	17.7
Number of coil blocks	35	35	9
Max. voltage (kV)	6.4	6.6	8.9

(2) The conductors are transferred to a reel of a winding machine. The reel revolves through the helical coil as shown in Fig. 7.

(3) The conductors are pulled aside by a set of winding guides and wound in grooves of the inner plate while being wrapped with glass tapes.

(4) After winding all turns in a layer, the next inner plates are assembled.

The torsion strain  $r\theta$  in winding is given as

$$r\theta = \frac{r \cdot \tan^{-1} \eta}{2\pi a_c/4}, \quad (8)$$

where  $r$  and  $\eta$  are the radius of the conductor and the lead angle of the helical coils, respectively. In the case of FFHR2m2 in Table 1, the strain is estimated at about 0.3%. If plastic forming of the conduit is required to settle it into the winding groove, extra torsion strain is neces-



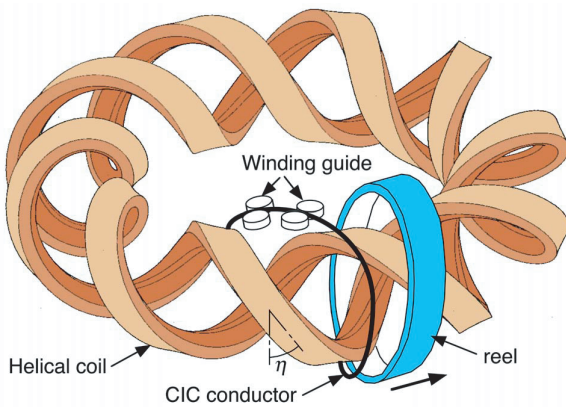


Fig. 7 Concept to wind a helical coil with CIC conductors.

sary. Since the effect of the torsion strain on the properties of superconducting strands is not known, a feasibility study is necessary. Thus, helical winding with CIC conductors requires the further development of technology for the ITER-TF coil.

#### 4. Poloidal Coil with CIC Conductors

The poloidal coils of LHD-type reactors are circular, similar to those of ITER. The typical design parameters of the poloidal coil of FFHR2m2 are listed in Table 4, compared with the largest poloidal field coil of ITER, PF3 coil. Since the radius of a larger coil, OV coil, is almost twice as large as the ITER-PF3 coil, parallel winding is also necessary. Although the coil current is large, the highest magnetic field can be lowered to a value less than 7 T by decreasing the coil current density. Therefore, NbTi strands can be adopted, and these coils are expected to be realized with the same technology as that for ITER.

#### 5. Summary

CIC conductors can be adopted for large helical windings by adopting layer winding and a parallel winding method. Since a react-and-wind method is preferred for large magnets, Nb<sub>3</sub>Al is a candidate for the helical coil conductor because of its good tolerance against mechanical strain. It is necessary to demonstrate the feasibility of its winding method. In addition, structural analyses of

Table 4 Specifications of poloidal coils with CIC conductors for FFHR2m2-γ1.20-γ27.5 (\*1).

	OV coil	IV coil	ITER-PF3
Radius of coils (m)	21.5	11.5	11.97
Number of coils	2	2	1
Coil current per coil, $I$ (MA)	19.6	12.1	8.46
Current density ( $A/mm^2$ )	15.3	16.8	15.26
Maximum field (T)	6.6	6.3	4
Turn number per layer	14	10	11.75
Layer number per coil	28	20	16
Conductor current (kA)	50.1	60.4	45
Length of a cooling path (m)	473	361	441.9
Number of parallel winding	4	2	2
Cu ratio of strand (-)	2	2	1
Non-Cu current density ( $A/mm^2$ )	200	200	230
Ratio of Cu strands in area (-)	0	0	0.24
Central tube diameter (mm)	12.0	12.0	12.0
Void fraction (-)	0.34	0.34	0.34
Cable outer diameter (mm)	40.1	43.7	34.5
Conduit height (mm)	55.1	58	52.3
Conduit width (mm)	55.1	58	52.3
Total length of conductor (km)	106	28.9	14.1
Total weight of SC strands (ton)	653	215	41.4
Total weight of conductor (ton)	2140	641	258

(\*1) The current density of the helical coil is  $27.5 A/mm^2$ .

the winding area are necessary to confirm the mechanical feasibility of the helical coils with a high current density of 25 to 30  $A/mm^2$ . This conceptual design is expected to be a conventional option that can be realized by a small extension from the ITER technology.

- [1] ITER Final Design Report, Magnet Superconducting Design Criteria, IAEA, Vienna, 2001.
- [2] N. Mitchell *et al.*, Fusion Eng. Des. **66-68**, 971 (2003).
- [3] A. Ulbricht *et al.*, Fusion Eng. Des. **73**, 189 (2005).
- [4] A. Sagara *et al.*, Nucl. Fusion **45**, 258 (2005).
- [5] S. Imagawa and A. Sagara, Plasma Sci. Technol. **7**, 2626 (2005).
- [6] H. Yamada *et al.*, Nucl. Fusion **45**, 1684 (2005).
- [7] S. Sudo *et al.*, Nucl. Fusion **30**, 11 (1990).
- [8] K. Okuno *et al.*, IEEE Trans. Appl. Supercond. **13**, 1437 (2003).
- [9] K. Kizu *et al.*, IEEE Trans. Appl. Supercond. **14**, 1535 (2004).
- [10] T. Takeuchi *et al.*, Appl. Phys. Lett. **71**, 122 (1997).
- [11] J.G. Weisend II, *Handbook of cryogenic engineering* (Taylor & Francis, 1998) p. 326.